AD-A070 044 DAVID W TAYLOR NAVAL SHIP RESEARCH AND DEVELOPMENT CE--ETC F/G 11/6
PREDICTION OF FATIGUE LIFE BY X-RAY DIFFRACTION METHODS.(U)
MAY 79 R N PANGBORN, S WEISSMANN, I R KRAMER

UNCLASSIFIED DTNSRDC-79/057 NL

| OF |
AD
A070044

END
DATE
FILMED
8-79
DDC

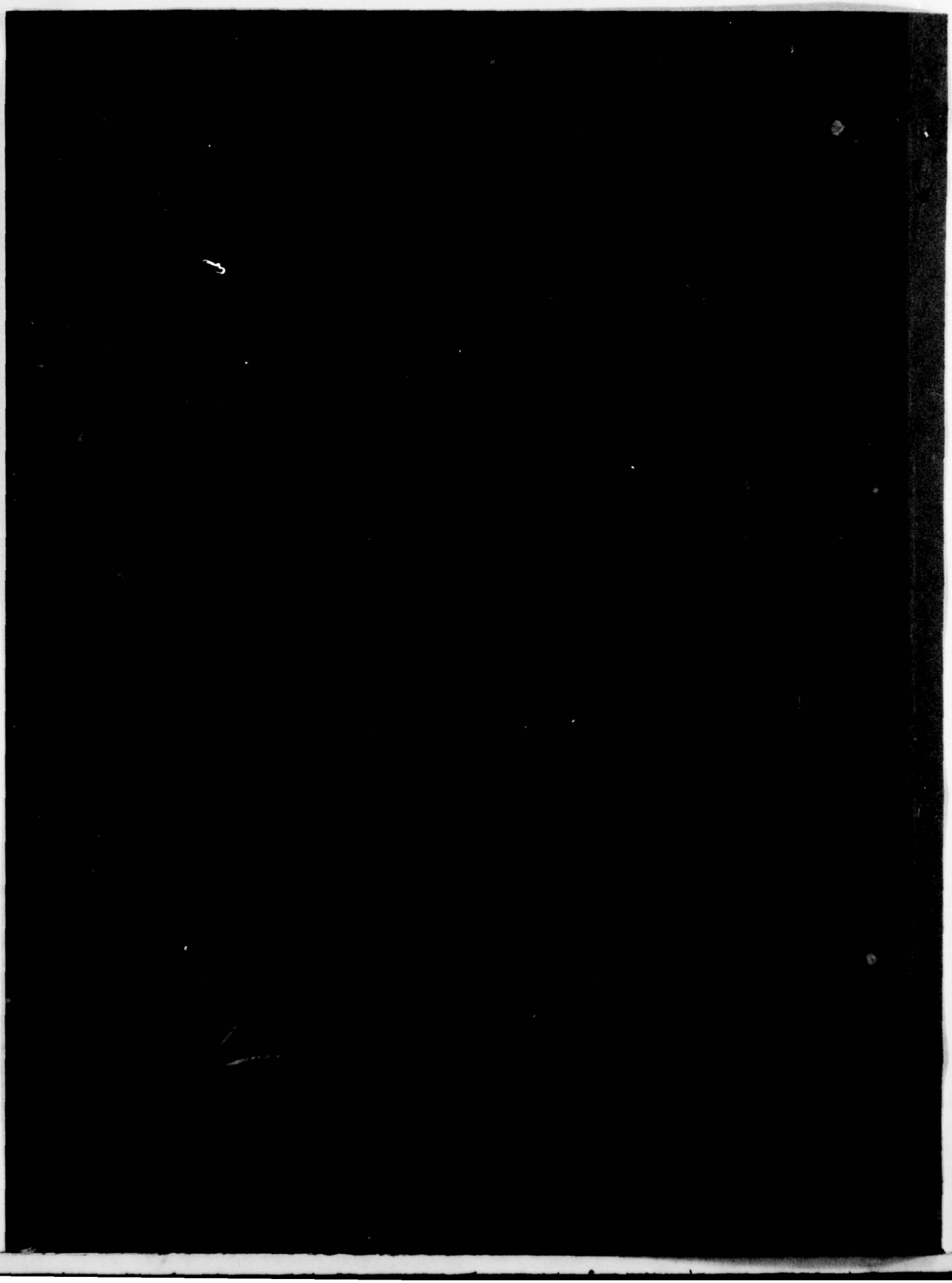

UNCLASSIFIED

SECURITY CLASSIFICATION OF THIS PAGE *(When Data Entered)*

REPORT DOCUMENTATION PAGE

READ INSTRUCTIONS BEFORE COMPLETING FORM

1. REPORT NUMBER: DTNSRDC-79/057	2. GOVT ACCESSION NO.
3. RECIPIENT'S CATALOG NUMBER	
4. TITLE *(and Subtitle)*: PREDICTION OF FATIGUE LIFE BY X-RAY DIFFRACTION METHODS.	5. TYPE OF REPORT & PERIOD COVERED: Research and Development Interim Report.
6. PERFORMING ORG. REPORT NUMBER	
7. AUTHOR(s): R.N. Pangborn and S. Weissmann (Rutgers University), and I.R. Kramer	8. CONTRACT OR GRANT NUMBER(s)
9. PERFORMING ORGANIZATION NAME AND ADDRESS: David W. Taylor Naval Ship R&D Center, Bethesda, Maryland 20084	10. PROGRAM ELEMENT, PROJECT, TASK AREA & WORK UNIT NUMBERS: Program Element 61152N; Task Area ZR 022-0101; Work Unit 2802-004
11. CONTROLLING OFFICE NAME AND ADDRESS: David W. Taylor Naval Ship R&D Center, Bethesda, Maryland 20084	12. REPORT DATE: May 1979
	13. NUMBER OF PAGES: 13
14. MONITORING AGENCY NAME & ADDRESS *(if different from Controlling Office)*	15. SECURITY CLASS. *(of this report)*: UNCLASSIFIED
	15a. DECLASSIFICATION/DOWNGRADING SCHEDULE

16. DISTRIBUTION STATEMENT *(of this Report)*

APPROVED FOR PUBLIC RELEASE: DISTRIBUTION UNLIMITED

17. DISTRIBUTION STATEMENT *(of the abstract entered in Block 20, if different from Report)*

18. SUPPLEMENTARY NOTES

19. KEY WORDS *(Continue on reverse side if necessary and identify by block number)*

Fatigue
X-ray diffraction
Aluminum

20. ABSTRACT *(Continue on reverse side if necessary and identify by block number)*

Through the use of a nondestructive X-ray method, the precrack fatigue damage in aluminum 2024-T3 has been determined. The method is based on (a) the observation that fatigue fracture is initiated when the excess dislocation density in the surface layer attains a critical value and (b) a knowledge of the excess-dislocation/depth profile for various fractions of fatigue damage. This profile indicates that if the X-ray radiation does not

(Continued on reverse side)

DD FORM 1 JAN 73 1473 EDITION OF 1 NOV 65 IS OBSOLETE
S/N 0102-LF-014-6601

UNCLASSIFIED
SECURITY CLASSIFICATION OF THIS PAGE *(When Data Entered)*

387 682

(Block 20 continued)

penetrate sufficiently deep into the surface layer, the dislocation density measurements cannot be used as a measurement of fatigue damage. By contrast, the application of penetrating molybdenum radiation, which irradiates grains in the bulk as well as in the surface, gives rise to a linear relationship between the X-ray linewidth and fatigue damage. The slope of this line is sufficiently steep so that, with a knowledge of the critical X-ray linewidth, the fatigue damage can be predicted. The fraction of fatigue damage is given by the ratio β/β^*, where β is the linewidth at any number of fatigue cycles and β^* is the critical linewidth at fracture. The critical linewidth may be estimated by using X-ray radiation from chromium and/or by a multiple film technique after the specimen has been cycled approximately 20 percent of its fracture life.

beta

Beta/Beta*

Beta*

TABLE OF CONTENTS

LIST OF FIGURES

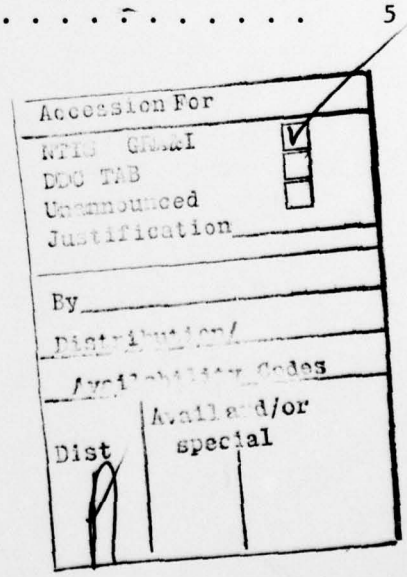

ABSTRACT

Through the use of a nondestructive X-ray method, the precrack fatigue damage in aluminum 2024-T3 has been determined. The method is based on (a) the observation that fatigue fracture is initiated when the excess dislocation density in the surface layer attains a critical value and (b) a knowledge of the excess-dislocation/depth profile for various fractions of fatigue damage. This profile indicates that if the X-ray radiation does not penetrate sufficiently deep into the surface layer, the dislocation density measurements cannot be used as a measurement of fatigue damage. By contrast, the application of penetrating molybdenum radiation, which irradiates grains in the bulk as well as in the surface, gives rise to a linear relationship between the X-ray linewidth and fatigue damage. The slope of this line is sufficiently steep so that, with a knowledge of the critical X-ray linewidth, the fatigue damage can be predicted. The fraction of fatigue damage is given by the ratio β/β^*, where β is the linewidth at any number of fatigue cycles and β^* is the critical linewidth at fracture. The critical linewidth may be estimated by using X-ray radiation from chromium and/or by a multiple film technique after the specimen has been cycled approximately 20 percent of its fracture life.

ADMINISTRATIVE INFORMATION

This investigation is part of an in-house research program at the David W. Taylor Naval Ship Research and Development Center. It was conducted under Program Element 61152N, Task Areas ZR 022-0101, Work Unit 2802-004.

INTRODUCTION

For many years X-ray diffraction patterns obtained from cyclically stressed metals and alloys have failed to provide neither clearcut indications of the impending onset of fatigue failure nor could they be used to predict, even approximately, the span of the fatigue life.[1,2*] Line

*A complete listing of references is given on page 9.

broadening was observed after cycling over a small fraction of the total fatigue life, but then it remained virtually unaltered both in extent and intensity throughout the remainder of the life.

A recent application of a special X-ray method[3,4] to cyclically stressed 2024 Al enabled the prediction of both the fatigue life and failure of the aluminum with a considerable degree of accuracy. This nondestructive method for analysis of the fatigue-induced defect structure is based on the principle of X-ray double-crystal diffractometry and employs X-ray topography to afford a visualization of the defect configuration. The polycrystalline specimen is irradiated with a crystal-monochromated beam, and each reflecting grain is considered to function independently as the test crystal of a double-crystal diffractometer. Depending on the perfection of the grains, the specimen is rotated in intervals of seconds or minutes of arc, and the spot reflections, recorded along the Debye arcs of a cyclidrical film for each discrete specimen rotation, are separated by film shifts. This multiple-exposure technique gives rise to an array of spots for each reflecting grain, as shown in Figure 1a. These arrays of spots, with their intensity dependent on specimen rotation, represent X-ray rocking curves of the reflecting grains. Thus, if the grains contain a substructure, the intensity distribution of the arrays of diffraction spots will be multipeaked, not only along the horizontal, but also along the

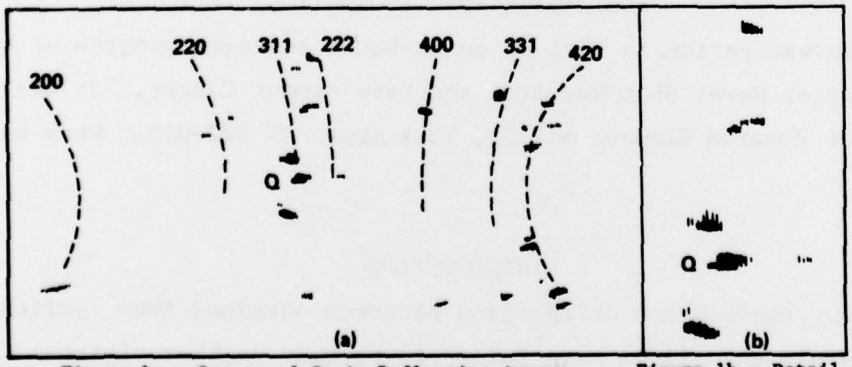

Figure 1a - Survey of Grain Reflection Arrays

Figure 1b - Detail of Reflection Range for Grain Q

Figure 1 - Rocking Curves of Grain Reflections of Fatigue-Cycled 2024 Al ($N = 10^4$). CuK_α Monochromated X-ray Radiation; Angular Specimen Setting 5 Minutes of Arc: Survey of Grain Reflections and Detail of Reflection Range for Grain Q

aximuthal elevation (Figure 1b). From the angle, subtending successive peaks of the rocking curve, the excess dislocation density between subgrains can be determined, while from the spread of the subpeak curve, the excess dislocation density within the subgrain lattice can be obtained. From the width β, at half the maximum of the rocking curve, the excess dislocation density of the entire grain is determined.[3,4]

The excess dislocation density D is calculated from the relationship given by Hirsch[5]

$$D = \beta^2/9b^2$$

where β is the width of the rocking curve at half of the intensity maximum (halfwidth) and b is the magnitude of the Burgers vector.

By analyzing various (hkl) reflections in this manner, a representative statistical parameter $\overline{\beta}$ of the defect structure of the grain population is obtained. Furthermore, by taking reflection topographs (Berg-Barrett) and performing a spatial tracing of the reflections to the spot reflections of the rocking curve, the analyzed rocking curve can be correlated to the grain topography on the specimen.[4]

The ability to predict the fatigue life of the Al alloy emerged from the results of a detailed study dealing with X-ray analysis of the work hardening in the surface layer and in the bulk during fatigue.[6] During the first halfcycle of fatigue, a surface layer was formed with a higher density of excess dislocations than that of the bulk material. On subsequent cycling, the density increased in the surface layer and, after about 5 percent of the fatigue life, a minimum began to appear in the depth profile. Further cycling increased the β values in the surface layer and in the bulk. The curves in Figure 2a show depth profiles for 2024 Al-T3 alloys fatigued to 75 percent and 95 percent of their life. The ratio β/β_o in Figure 2 represents the average rocking curve width of the grains normalized with respect to the width value prior to fatigue. Similar to the depth profile previously obtained for an Al single crystal strained in tension,[7] β was highest at the surface up to a depth of about 100 μm. Beyond this depth, β increased and attained a constant value at about

250 μm into the bulk. The value for β in the interior increased with the number of fatigue cycles but never exceeded that at the surface.

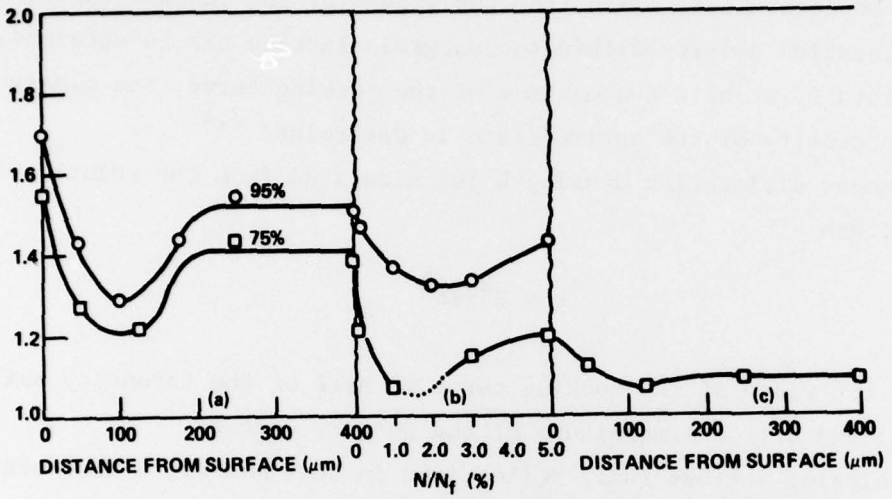

Figure 2a - Surface Layer Removal

Figure 2b - Recycling to $N/N_F = 0.05$

Figure 2c - Surface Layer Removal

Figure 2 - Complete Diagram for 2024 Al given Prior Fatigue Cycling to 95 Percent and 75 Percent of Fatigue Life Followed by: Surface Layer Removal, Recycling to $N/N_F = 0.05$, and Surface Layer Removal

It has been reported previously[8] that during uniaxial fatigue cycling, as in unidirectional tensile tests[9,10], the surface layer work hardens more rapidly than that of the bulk material. A systematic investigation[11] of 2014 Al-T6, Ti-6Al-4V, and a 4130 steel showed that a propagating fatigue crack was formed whenever the work hardening in the surface layer reached a critical value. This critical value was independent of the stress amplitude, prior fatigue history, and environment. It was proposed[11] that the surface layer acted to oppose the motion of dislocations by providing a barrier to support a piled-up array of dislocations of like sign. When the barrier becomes sufficiently strong, fracture occurs when the local stress field associated with an accumulation of excess dislocations exceeds the fracture strength. In agreement with the concept of Kramer[11] and the data of Taira et al.[12], the rocking curve data showed that fatigue fracture occurred at a constant β value equal to about 70 minutes of arc ($D - 6 \times 10^{10}/cm^2$); this critical β value was independent of the cyclic stress amplitude.

The approach toward this critical β value cannot be predicted with certainty if the X-ray radiation employed does not penetrate sufficiently deep into the work-hardened surface layer. As may be seen from Figure 3, application of CuK_α radiation, which penetrates only a portion of the work-hardened surface layer, gave rise to a rapid increase of β/β_o between N/N_F = 0 and 20 percent, but from 20 percent to 90 percent the increase was very gradual, having nearly a plateau appearance.* Beyond N/N_F = 90 percent, β/β_o becomes critical and leads rapidly to fracture at $(\beta/\beta_o)^*$. By contrast, application of the penetrating molybdenum radiation, which irradiated grains in the bulk as well as those in the surface layer, gave rise to a straight line that had a pronounced slope up to the critical value $(\beta/\beta_o)^*$. The slope was sufficiently steep so that, with the aid of a calibration curve and its error band, $(\beta/\beta_o)^*$ could be predicted at various stages of N/N_F.

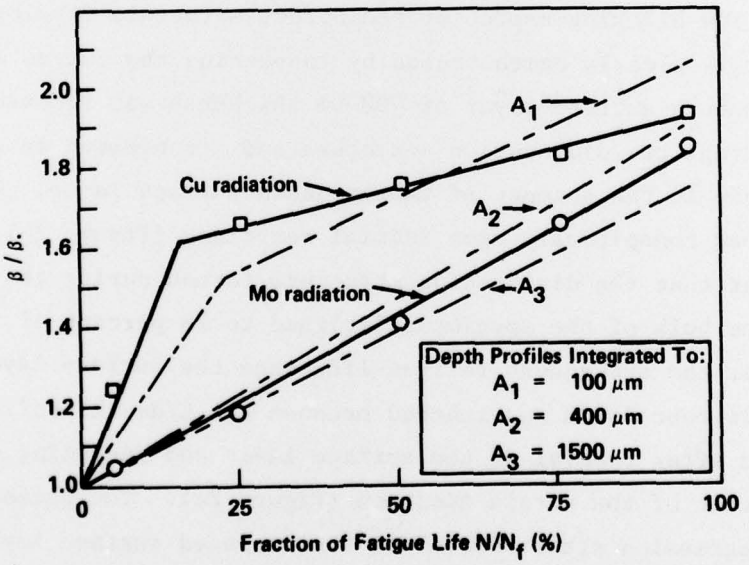

Figure 3 - Dependence of Rocking Curve Width of Surface Layer and Bulk on Fatigue Cycling for Al 2024-T3

*N = number of fatigue cycles; N_F = number of fatigue cycles to fracture.

The steep, single-stage curve resulted from the added contribution of the defect structure in the bulk. This is revealed by Figure 3 which shows the molybdenum data in conjunction with a plot of the areas under the depth profiles as a function of N/N_F. Indeed, the curves obtained by integration of the depth profiles to depths of 400 and 1500 μm can be drawn to virtually coincide with that obtained experimentally using molybdenum radiation. In contrast, integration to only 100 μm from the surface provided a three-stage curve similar to that derived by analysis with shallow-penetrating copper radiation.

Our studies have now made it evident why in the past the X-ray patterns of cycled specimens were inconclusive in predicting fatigue failure. For virtually the entire fatigue life, the rapidly-work-hardened surface layer blocks the egression of dislocations from the bulk. If the X-ray radiation does not penetrate beyond this surface layer, the slight increase of β (or X-ray line broadening) falls well within the experimental error band. The blocking aspect of the defect structure developed in the surface layer is clearly demonstrated by inspecting the curves of Figures 2b and 2c. When a surface layer of 400-μm thickness was removed by electropolishing, the dislocation structure and arrangement in the bulk became unstable in the absence of the hardened surface layer. The β/β_o values declined conspicously upon initial recycling (Figure 2b). It also became evident that the dislocation structure formed during the fatigue process in the bulk of the specimen, fatigued to 75 percent of its life, did not impair the subsequent fatigue life once the surface layer was removed. This conclusion was reached because the β/depth profile after fatiguing and after removal of the surface layer and recycling was nearly the same as that of the virgin specimen (Figure 2c). The phenomenon of dislocation egression after removal of the hardened surface layer and concomitant strain relief explain why the fatigue life of a material can be extended almost indefinitely if the surface layers are judiciously removed, as previously found by Thompson et al.[13] and by Kramer.[11] The remarkable extension of fatigue life resulting from surface removal is ascribed, therefore, not to the removal of microcracks, but principally to the removal of the blocking effect of the hardened surface layer.

In practice, the β/β_o values for the surface layer plus bulk, and for the surface layer alone, can be obtained by carrying out a simple exposure sequence using MoK_α radiation. The reflections are recorded on multiple films separated by copper foils of appropriate thickness. The first film records the contribution of surface layer and bulk, but the second film, owing to the suppression of the weak intensities by the interposed copper screen, registers only the intense reflections emanating from the surface layer. In this way, fatigue failure prediction can be accomplished quickly, accurately, and nondestructively.

REFERENCES

1. Bennett, J.A., J. Research Natl. Bur. Standards, 46, 457 (1951).

2. Love, W.J., "Structural Changes in Ingot Iron Caused by Plastic and Repeated Stressing." Project NR-031-005, Dept. T.A.M. University of Illinois (Sep 1952).

3 Weissmann, S. and D.L. Evans, Acta Cryst., 7, 733 (1954).

4. Weissmann, S., J. Appl. Phys., 27, 389 (1956).

5. Hirsch, P.B., "Mosaic Structure," Prog. Met. Phys., 6, 283 (1956).

6. Pangborn, R.N., S. Weissmann, and I.R. Kramer, Scripta Metallurgica, 12, 129 (1978).

7. Pangborn, R.N., A. Gysler, and S. Weissmann, Second International Conference on Mechanical Behavior Of Materials, (16-20 Aug 1976) p. 1746.

8. Kramer, I.R., Proc. Air Force Conference on Fatigue, AFFDL-TR-70-144 (1969).

9. Kramer, I.R. and L.J. Demer, Trans. TMS-AIME, 227, 1003 (1963).

10. Kramer, I.R., Trans. TMS-AIME, 230, 991 (1964).

11. Kramer, I.R., Met. Trans., 5, 1735 (1974).

12. Taira, S., K. Tanaka, and T. Tanabe, Proc. 13th Japanese Congress on Materials Research (1970) pp. 14-19.

13. Thompson, N.T., N.J. Wadsworth, and N. Louat, Phil. Mag., 1, 113 (1956).

INITIAL DISTRIBUTION

Copies		
2	CNR	
	1	Code 465
	1	Code 471
6	NRL	
	1	Code 6000
	5	Code 6300
6	NAVSEA	
	1	SEA 035
	1	SEA 05D
	2	SEA 323
	2	SEA 99632
12	DDC	

CENTER DISTRIBUTION

Copies	Code	Name
2	012	
1	012.1	
2	17	
1	28	
1	280	
15	2802	
2	281	
6	282	
10	5211.1	Reports Distribution
1	522.1	Library (C)
1	522.2	Library (A)
2	5231.2	Office Services